Title

Optical coherence tomography as a possible tool to monitor and predict disease progression in mitochondrial myopathy, encephalopathy, lactic acidosis and stroke-like episodes

Authors' names and email addresses

Akihiro Shinkai, shinkai@huhp.hokudai.ac.jp;

Yasuhiro Shinmei, yshinmei@med.hokudai.ac.jp;

Kiriko Hirooka, hirooka0516@huhp.hokudai.ac.jp;

Yoshiaki Tagawa, yocchinn0127@med.hokudai.ac.jp

Kayoko Nakamura, chibichibitank555@gmail.com;

Shinki Chin, schin@med.hokudai.ac.jp;

Susumu Ishida, ishidasu@med.hokudai.ac.jp

Authors' affiliation

Department of Ophthalmology, Faculty of Medicine and Graduate School of Medicine, Hokkaido University, N-15, W-7, Kita-ku, Sapporo 060-8638, Japan

Correspondence to: Yasuhiro Shinmei, M.D., Ph.D.

Department of Ophthalmology, Faculty of Medicine and Graduate School of Medicine,

Hokkaido University, N-15, W-7, Kita-ku, Sapporo 060-8638, Japan

Phone: +81-11-706-5944, Fax: +81-11-706-5948, E-mail: yshinmei@med.hokudai.ac.jp

Abstract

Optical coherence tomography (OCT) is an imaging technique used to obtain three-dimensional information on the retina. In this article, we evaluated the structural neuro-retinal abnormalities, especially the thickness in the ganglion cell complex (GCC), in patients with mitochondrial myopathy, encephalopathy, lactic acidosis and stroke-like episodes (MELAS). The GCC thickness in MELAS patients was significantly thinner than that in normal controls even when they had no history of transient homonymous hemianopia. There was a negative correlation between GCC thickness and disease duration. In conclusion, OCT may be an effective tool to monitor and predict disease progression in MELAS patients.

Keywords

Mitochondrial myopathy, encephalopathy, lactic acidosis and stroke-like episodes

Optical coherence tomography

Leber hereditary optic neuropathy

Ganglion cell complex

homonymous hemianopia

Highlights

- This was a study using the optical coherence tomography (OCT) imaging technique in MELAS patients to obtain three-dimensional information on the retina.
- The GCC thickness in MELAS patients was significantly thinner than that in normal controls even when they had no history of transient homonymous hemianopia.
- These GCC changes were associated with the disease duration.
- This study suggested that OCT is an effective tool to monitor and predict disease progression in MELAS patients.

1. Introduction

Defects in complex I due to mutations in mitochondrial DNA are associated with clinical features ranging from single organ manifestations like Leber hereditary optic neuropathy (LHON) to multi-organ disorders like mitochondrial myopathy, encephalopathy, lactic acidosis and stroke-like episodes (MELAS) syndrome (Ng and Turnbull, 2016). The progress of MELAS primarily affects muscles and the central nervous system, including the visual pathways (El-Hattab et al., 2015). Energy failure due to faulty mitochondria is a common feature of mitochondrial diseases, in addition to the overproduction of reactive oxygen species (ROS) (Indo et al., 2007). The eye is frequently affected, along with the skeletal muscles, brain and heart because of their high energy requirements (Lefevere et al., 2017).

Rummelt et al. described the histopathological findings in two eyes obtained at autopsy from a 21-year-old woman with MELAS (Rummelt et al., 1993). Ragged-red fibers in the rectus muscles, degeneration of photoreceptor outer segments in the macula, hyperpigmentation and atrophy of the retinal pigment epithelium of the macula, atrophy of the iris stroma, early posterior subcapsular cataract and optic atrophy were all observed.

Although vision loss due to cortical vision loss, pigmentary retinopathy and/or optic nerve atrophy may occur in MELAS patients, ophthalmic involvement in the disease has not been thoroughly evaluated *in vivo* using modern retinal imaging techniques. To the best of our knowledge, there are only a few case reports of patients with MELAS using optical coherence tomography (OCT) (Cho and Yu, 2015; Daruich et al., 2014; Mack et al., 2018; Navajas and Xu, 2015). However, the entire clinical picture is not clear on the basis of a case series.

The aim of our study was to evaluate structural neuro-retinal abnormalities, especially the thickness of the ganglion cell complex (GCC), in patients with MELAS in comparison with normal controls and patients with LHON. GCC contains the axons, cell bodies and dendrites of ganglion cells, and is a diagnostic parameter in several optic nerve diseases, including glaucoma. Next, we investigated the relationship between disease duration and OCT findings in MELAS patients for assessing OCT measurements as a biomarker. We also compared the differences in OCT images between the groups with and without a history of transient homonymous hemianopia to investigate the association between their OCT abnormalities and functional impairments.

2. Materials and methods

2.1. Patients and controls

This retrospective observational case series involved 5 patients with MELAS. Five patients with LHON and 5 age-matched normal subjects were used as controls. The patients were referred to the Department of Ophthalmology, Hokkaido University Hospital between January 2016 and March 2020. Participants were excluded if they had spherical refractive error less than -5 diopters (D) or more than +5 D, intraocular pressure (IOP) greater than 22 mmHg, retinal and retinal pigment epithelium (RPE) degeneration, co-existing confounding ocular disease or history of any retinal surgery. The clinical data are summarized in the Table. All patients with MELAS had normal visual acuity. The visual field defects in 2 out of 5 MELAS patients were homonymous hemianopia with macular sparing when they developed temporo-occipital cortex lesions. While in all 5 patients with LHON, visual field testing consistently revealed bilateral

central scotoma. In 2 MELAS patients with visual field defect, the visual acuities had been normal (average logMAR was 0.02 ± 0.02) during homonymous hemianopia and after recovery because of their macular sparing. End-stage MELAS patients and those with pigmentary retinopathy were not included in this study. Their scores on the Japanese Mitochondrial Disease Rating Scale (Yatsuga et al., 2012) were less than one point for each item. The disease duration means the period after the first stroke-like attack in MELAS or the first onset of optic neuropathy in LHON. There was no significant difference in gender, age, spherical equivalent or visual acuity between the MELAS group and normal controls (Mann-Whitney U test, chi-square test: $p<0.05$).

The study was compliant with the Health Insurance Portability and Accountability Act and adhered to the tenets of the Declaration of Helsinki. It was reviewed and approved by the institutional review board of Hokkaido University Hospital and Hokkaido Medical Center for clinical research (#020-0025), and informed consent was received from all participants.

Table. Characteristics of patients and controls

		MELAS	LHON	Normal controls
Patients	no.	5	5	5
Eyes	no.	10	10	10
Gender	Male	2	3	2
	Female	3	2	3
Age (Years)	Mean	29.8	41.8	32.0
	SD	8.3	8.5	2.5
Spherical equivalent	Mean	-1.8	0.0	-1.8
(Dioptors)	SD	1.3	0.9	1.5
VA (LogMAR score)	Mean	-0.06	1.31	-0.13
	SD	0.09	0.47	0.05
Gene mutation	mt3243A>G	4	-	-
	mt3258T>C	1	-	-
	mt11778G>A	-	5	-
Disease duration (Months)	Mean	152.6	178.8	-
	SD	160.7	120.8	-
Visual field defect	no. (%)	4 (40%)	10 (100%)	-

MELAS; mitochondrial encephalomyopathy, lactic acidosis, and stroke-like episodes, LHON; Leber hereditary optic neuropathy, VA; best-corrected visual acuity, SD; standard deviation.

2.2. Investigations

2.2.1. Ophthalmic examinations

All patients and control participants underwent thorough ophthalmic examinations in order to exclude ocular pathology possibly confounding the OCT analysis. These included measurement of the best-corrected visual acuity (VA), refractive error and IOP; slit-lamp biomicroscopy, fundus examination and visual field test. Their data including medical history were also collected retrospectively.

2.2.2. OCT analysis

The retinal thickness was measured with spectral domain OCT (RS-3000 Advance®; software version 1.5.5.0; Nidek, Gamagori, Japan) using glaucoma analysis software in all participants. OCT has an axial depth resolution and transverse resolution values of 7 μm and 20 μm, respectively. Raster scans over a 9 × 9-mm^2 area centered on the fovea center with a scan density of 512 A-scans × 128 B-scans were acquired for each subject. Individual data sets were acquired within 1.6 seconds. The scanned data were digitally exported and the average GCC thickness was assessed using the built-in software with RS-3000 Advance automatically. GCC thickness was measured between the internal limiting membrane (ILM) and the outer boundary of the inner plexiform layer (IPL)(Giraud et al., 2014).

We also assessed the outer retinal complex (ORC) thickness, excluding the GCC, measured between the inner nuclear layer (INL) and RPE for comparison (Chan et al., 2006). The ORC contains the outer nuclear layer and inner and outer segments of the photoreceptor cells, and thinning is considered to reflect photoreceptor degeneration. Images with incorrect segmentation or other inappropriate data were excluded and only high-quality images with

"Signal Strength Index" scores of at least 6/10 were included in the analysis (Morooka et al., 2012).

2.2.3. Statistical analysis

All results were expressed as the mean ± standard deviation (SD). Statistical analyses were performed using Mann-Whitney U test, Kruskal-Wallis test and the chi-square test. Correlation analysis was performed with Spearman's rank correlation coefficient as appropriate. A *p*-value below 0.05 was considered significant.

3. Results

3.1. Glaucoma analysis map on OCT

As a representative case, we presented the OCT of a 24-year-old woman with optically asymptomatic MELAS (Figure 1). She was genetically diagnosed with MELAS (mt3243A>G) at 20 years of age. She had had stroke-like seizures, but no abnormalities were detected in her visual acuity or visual field. The scan analysis was performed and delivered to 3 maps: a thickness map, a deviation map and a thickness compared with normative database map. The red area in the normative database map (< 1% probability of being within the normal range) indicates an area of decreased GCC thickness. Each value in the GChart or S/I represents the GCC thickness of each segmented area. Next, we compared the GCC thickness in the macula area based on these values.

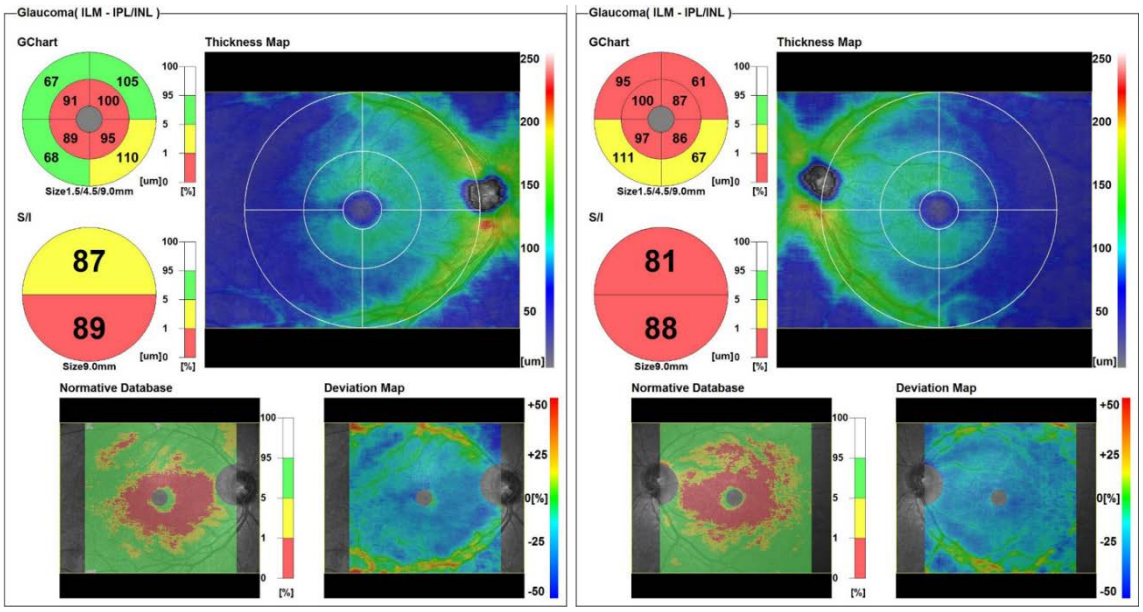

Figure 1. Glaucoma analysis map on OCT

Fovea-centered OCT of the macular cube (512 A-scans × 128 B-scans) with automatic segmentation (GChart and S/I) and color-coded thickness compared with normative database and deviation maps of GCC thickness, which was measured between ILM and IPL/ INL boundary by the embedded program.

3.2. Stratified quantitative analysis on OCT

Box and whisker plots comparing the average GCC thickness among controls, MELAS, and LHON groups are shown in Figure 2. GCC thickness was measured from the ILM to IPL/INL boundary, which supplements the clinical work-up for the early detection of optic nerve fiber layer defects.

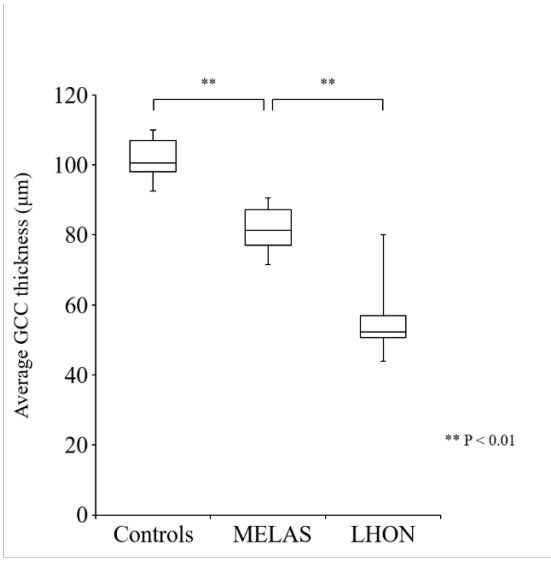

Figure 2. Box and whisker plots comparing the average GCC thickness among the control, MELAS, and LHON groups

GCC thickness was compared among the control, MELAS, and LHON groups using the nonparametric Kruskal-Wallis test and Mann-Whitney U test. There was a significant difference among the three groups ($p<0.0001$), between the control and MELAS groups ($p<0.0001$), and between the MELAS and LHON groups ($p=0.0002$). The rectangular box represents the 75th and 25th percentiles of the data, and the horizontal line is the median. The vertical lines show the range.

There was a significant difference in GCC thickness among the MELAS, LHON, and control groups ($p < 0.0001$). The GCC thickness of the MELAS group was significantly thinner than that of controls, but significantly thicker than that of the LHON group ($p < 0.0001$, $p = 0.0002$, respectively). The maximum values were 110.0, 90.5 and 80.0, the 75th percentiles were 106.9,

87.1 and 56.9, the medians were 100.5, 81.3 and 52.3, the 25th percentiles were 98.0, 77.1 and 50.8, and the minimum values were 92.5, 71.5 and 44.0 in the control, MELAS and LHON groups, respectively (mean ±SD: 101.8 ± 5.5, 81.6 ± 6.4 and 55.1 ± 9.9, respectively).

On the other hand, there was no significant difference among the control, MELAS, and LHON groups in ORC thickness, which reflected the structural change of photoreceptor cells (Kruskal-Wallis test, p = 0.86; mean ± SD: 190.3 ± 5.1, 188.1 ± 1.5 and 190.7 ± 9.1, respectively) (Figure 3).

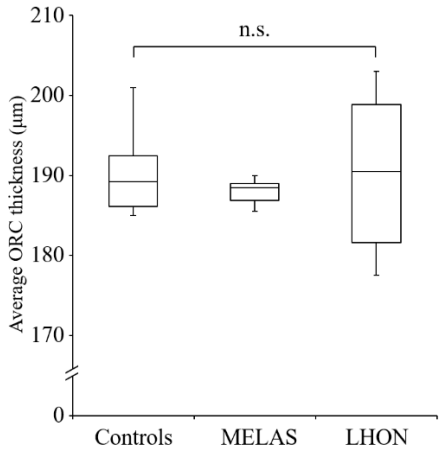

Figure 3. Box and whisker plots comparing the average ORC thickness among the control, MELAS, and LHON groups

ORC thickness was compared among the control, MELAS, and LHON groups using the nonparametric Kruskal-Wallis test. There was no significant difference among the three groups (p=0.86). The rectangular box represents the 75th and 25th percentiles of the data, and the horizontal line is the median. The vertical lines show the range. The maximum values were

201.0, 190.0 and 203.0, the 75th percentiles were 192.5, 189.0 and 198.9, the medians were 189.3, 188.5 and 190.5, the 25th percentiles were 186.1, 186.9 and 181.6, and the minimum values were 185.0, 185.5 and 177.5 in the control, MELAS, and LHON groups, respectively (mean ± SD: 190.3 ± 5.1, 188.1 ± 1.5 and 190.7 ± 9.1, respectively).

3.3. The relationship between disease duration and GCC thickness in MELAS patients

We next investigated the relationship between disease duration and GCC thickness in MELAS patients. A scatter-plot demonstrating a negative correlation between GCC thickness and disease duration in the MELAS group is shown in Figure 4 (Spearman's rank correlation coefficient, $\rho = -0.76$, $p = 0.01$). These include the data measured for each eye of each patient (n=10).

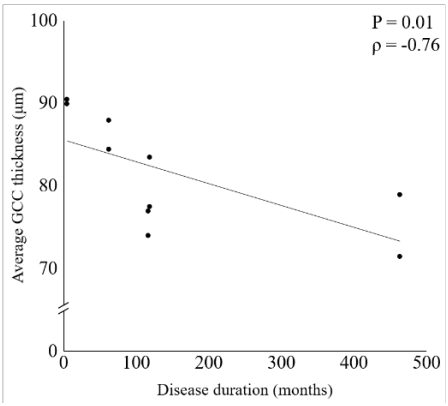

Figure 4. Scatter-plot of disease duration and GCC thickness in MELAS patients

A negative correlation between disease duration and GCC thickness was observed (Spearman's rank correlation coefficient $\rho = -0.76$, $p < 0.01$, n=10 eyes).

3.4. GCC thickness in MELAS patients with and without a history of transient homonymous hemianopia

Furthermore, we compared GCC thickness between the MELAS patients with and without a history of transient homonymous hemianopia to investigate its association with their OCT abnormalities. Box and whisker plots comparing GCC thickness between the groups are shown in Figure 5 (mean ± SD: 82.9 ± 7.5, 80.7 ± 5.4, respectively). There was no significant difference in GCC thickness between the two groups (P=0.76).

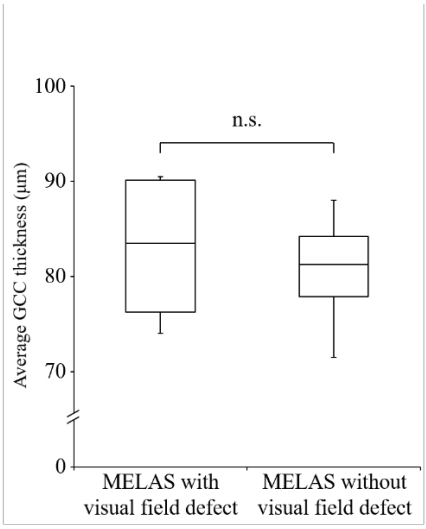

Figure 5. Box and whisker plots comparing GCC thickness between MELAS patients with and without visual dysfunction

Six of 10 eyes had no history of visual dysfunction (MELAS without visual dysfunction). Four of 10 eyes had visual field defects or a history of defects. There was no significant difference between the two groups (Mann-Whitney U test: p=0.76).

4. Discussion

OCT is an imaging technique similar to ultrasound, except that optical rather than acoustic reflectivity is measured (Puliafito et al., 1995). One-dimensional A-scans are obtained and two-dimensional images (B-scans) are constructed. Cross-sectional B-scans provide three-dimensional information. This technique has changed diagnostics in ophthalmology enabling visualization of high-resolution morphology of retinal cell layers, which play an important role in human vision (Renard et al., 2019).

Analyses of retinal cell layers have led to major breakthroughs in neurodegenerative diseases. Previous studies suggested that OCT parameters can predict disability progression and visual function in patients with multiple sclerosis (Britze and Frederiksen, 2018). Furthermore, multiple studies have demonstrated the benefits of these advancements, particularly in Alzheimer's disease (Doustar et al., 2017), Parkinson's disease (Satue et al., 2013) and Huntington's disease (Kersten et al., 2015), none of which are usually accompanied by visual dysfunction. Similar results were suggested in visually asymptomatic patients with genetically confirmed myoclonic epilepsy with ragged-red fibers syndrome (Najjar et al., 2019).

In our study, all the 10 eyes of 5 patients with genetically confirmed MELAS had neuro-retinal abnormalities affecting the macular GCC based on OCT. The thickness was significantly

thinner than that in age-matched normal controls, but thicker than that in LHON patients. However, there was no significant difference in ORC thickness among the three groups. This suggested that retinal ganglion cell (RGC) death subclinically progresses even in MELAS patients with normal visual function, whereas photoreceptor cells were relatively undisturbed in both diseases. RGC death in MELAS patients being milder than that in patients with LHON may explain why their visual function was maintained compared with that in patients with LHON.

To our knowledge, there are four previous studies on retinal changes in patients with MELAS by OCT. Cho et al. reported an 11-year-old male patient with MELAS who had transient left homonymous hemianopsia and defects of the nasal retinal nerve fiber layer, which is a main component of the GCC, in both eyes, neither of which was correlated with the brain lesion (Cho and Yu, 2015). On the other hand, Mack et al. reported a 50-year-old male patient with MELAS who developed transient bilateral optic disc edema followed by spontaneous full recovery, without the subsequent development of optic nerve atrophy on OCT (Mack et al., 2018). Our results are consistent with Cho's case, and support their suggestion that OCT is a useful tool to detect optic atrophy in patients who have mitochondrial disease and normal morphology of the optic nerve head. The conflicting results of the two reports may be explained by the disease duration. In our study, there was a negative correlation between GCC thickness and disease duration in MELAS patients. This suggests that RGC degeneration may develop gradually over time in patients with MELAS. In addition, Navajas et al. observed outer retinal tubulations within areas of RPE atrophy in a 40-year-old female patient with MELAS who had progressive visual loss and pigmentary retinopathy using OCT (Navajas and Xu, 2015) . Similarly, Daruich et al. reported two cases of MELAS with variable degrees of RPE changes

(Daruich et al., 2014). Their patients had a long disease duration, which may be related to the severity of systemic and ocular phenotypes. The ocular histopathological findings of MELAS such as degeneration of photoreceptor outer segments, hyperpigmentation and atrophy of RPE, and optic atrophy (Rummelt et al., 1993) may only be observed in patients with advanced disease. Our patients did not exhibit such outer retinal or RPE lesions, and there was no significant difference between our patients and controls in ORC thickness, possibly because we initially excluded patients with funduscopic retinal lesions. Even in patients with MELAS who have no ocular symptoms at examination, as the RGC disorder progresses, optic nerve atrophy will occur in the future, resulting in decreased visual acuity. Thinning of the GCC may precede photoreceptor damage.

Next, we considered the possibility that cortical blindness may retrogradely reduce RGCs. Lesions in the posterior visual pathways via trans-synaptic degeneration may lead to the loss of RGCs. However, there was no significant difference in the thickness of the inner layer of the retina between the groups with and without a history of cortical blindness. Based on this, the decrease in RGCs may reflect subclinical structural damage before visual impairment. As another possibility, MELAS/LHON overlaps were rarely reported (Blakely et al., 2005; Hsieh et al., 2011; Pätsi et al., 2012). All of our patients with MELAS had normal visual acuity at the examination; therefore, it is unlikely that LHON overlapped.

The eye is the only part of the central nervous system readily accessible for both measurement and therapeutic strategies aimed to protect against neurodegeneration. The eye will likely provide a window for major breakthroughs in the management of neurodegenerative diseases. OCT may be an effective tool to monitor and predict disease progression in MELAS patients.

This study has several limitations. The sample size was small due to rarity of the diseases. The genetic background was not homogenous in our MELAS patients. The relationship with the mtDNA heteroplasmy was not clear. Further studies with a larger sample size and longer follow-up period at multiple centers are required to confirm the findings of our present study.

Funding

This study did not receive any specific grant from funding agencies in the public, commercial or not-for-profit sectors.

Disclosure of conflicts of interest

None of the authors have any conflicts of interest to disclose.

Acknowledgements

None.

References

Blakely, E.L., de Silva, R., King, A., Schwarzer, V., Harrower, T., Dawidek, G., Turnbull, D.M., and Taylor, R.W. (2005). LHON/MELAS overlap syndrome associated with a mitochondrial MTND1 gene mutation. Eur J Hum Genet *13*, 623-627.

Britze, J., and Frederiksen, J.L. (2018). Optical coherence tomography in multiple sclerosis. Eye (Lond) *32*, 884-888.

Chan, A., Duker, J.S., Ishikawa, H., Ko, T.H., Schuman, J.S., and Fujimoto, J.G. (2006). Quantification of photoreceptor layer thickness in normal eyes using optical coherence tomography. Retina *26*, 655-660.

Cho, K.J., and Yu, J. (2015). Retinal nerve fibre layer defect associated with MELAS syndrome. Can J Ophthalmol *50*, e85-88.

Daruich, A., Matet, A., and Borruat, F.X. (2014). Macular dystrophy associated with the mitochondrial DNA A3243G mutation: pericentral pigment deposits or atrophy? Report of two cases and review of the literature. BMC Ophthalmol *14*, 77.

Doustar, J., Torbati, T., Black, K.L., Koronyo, Y., and Koronyo-Hamaoui, M. (2017). Optical Coherence Tomography in Alzheimer's Disease and Other Neurodegenerative Diseases. Front Neurol *8*, 701.

El-Hattab, A.W., Adesina, A.M., Jones, J., and Scaglia, F. (2015). MELAS syndrome: Clinical manifestations, pathogenesis, and treatment options. Mol Genet Metab *116*, 4-12.

Giraud, J.M., El Chehab, H., Francoz, M., Fenolland, J.R., Delbarre, M., May, F., and Renar, J.P. (2014). Optical Coherence Tomography in the Inner Retinal Layers. In Optical Coherence Tomography ESASO Course Series, G. Coscas, A. Loewenstein, and F. Bandello, eds. (Basel: Karger), pp. 17-25.

Hsieh, Y.T., Yang, M.T., Peng, Y.J., and Hsu, W.C. (2011). Central retinal vein occlusion as the initial manifestation of LHON / MELAS overlap syndrome with mitochondrial DNA G13513A mutation--case report and literature review. Ophthalmic Genet *32*, 31-38.

Indo, H.P., Davidson, M., Yen, H.C., Suenaga, S., Tomita, K., Nishii, T., Higuchi, M., Koga, Y., Ozawa, T., and Majima, H.J. (2007). Evidence of ROS generation by mitochondria in cells with impaired electron transport chain and mitochondrial DNA damage. Mitochondrion *7*, 106-118.

Kersten, H.M., Danesh-Meyer, H.V., Kilfoyle, D.H., and Roxburgh, R.H. (2015). Optical coherence tomography findings in Huntington's disease: a potential biomarker of disease progression. J Neurol *262*, 2457-2465.

Lefevere, E., Toft-Kehler, A.K., Vohra, R., Kolko, M., Moons, L., and Van Hove, I. (2017). Mitochondrial dysfunction underlying outer retinal diseases. Mitochondrion *36*, 66-76.

Mack, H.G., Milea, D., Thyagarajan, D., and Fagan, X. (2018). Transient bilateral optic disc oedema in mitochondrial encephalomyopathy, lactic acidosis, and stroke-like episodes (MELAS). Can J Ophthalmol *53*, e208-e211.

Morooka, S., Hangai, M., Nukada, M., Nakano, N., Takayama, K., Kimura, Y., Akagi, T., Ikeda, H.O., Nonaka, A., and Yoshimura, N. (2012). Wide 3-dimensional macular ganglion cell complex imaging with spectral-domain optical coherence tomography in glaucoma. Invest Ophthalmol Vis Sci *53*, 4805-4812.

Najjar, R.P., Reynier, P., Caignard, A., Procaccio, V., Amati-Bonneau, P., Mack, H., and Milea, D. (2019). Retinal Neuronal Loss in Visually Asymptomatic Patients With Myoclonic Epilepsy With Ragged-Red Fibers. J Neuroophthalmol *39*, 18-22.

Navajas, E.V., and Xu, K. (2015). Spectral-domain optical coherence tomography in mitochondrial encephalopathy, lactic acidosis, and strokelike episodes. Can J Ophthalmol *50*, e115-117.

Ng, Y.S., and Turnbull, D.M. (2016). Mitochondrial disease: genetics and management. J Neurol *263*, 179-191.

Puliafito, C.A., Hee, M.R., Lin, C.P., Reichel, E., Schuman, J.S., Duker, J.S., Izatt, J.A., Swanson, E.A., and Fujimoto, J.G. (1995). Imaging of macular diseases with optical coherence tomography. Ophthalmology *102*, 217-229.

Pätsi, J., Maliniemi, P., Pakanen, S., Hinttala, R., Uusimaa, J., Majamaa, K., Nyström, T., Kervinen, M., and Hassinen, I.E. (2012). LHON/MELAS overlap mutation in ND1 subunit of mitochondrial complex I affects ubiquinone binding as revealed by modeling in Escherichia coli NDH-1. Biochim Biophys Acta *1817*, 312-318.

Renard, J.P., Fénolland, J.R., and Giraud, J.M. (2019). Glaucoma progression analysis by Spectral-Domain Optical Coherence Tomography (SD-OCT). J Fr Ophtalmol *42*, 499-516.

Rummelt, V., Folberg, R., Ionasescu, V., Yi, H., and Moore, K.C. (1993). Ocular pathology of MELAS syndrome with mitochondrial DNA nucleotide 3243 point mutation. Ophthalmology *100*, 1757-1766.

Satue, M., Garcia-Martin, E., Fuertes, I., Otin, S., Alarcia, R., Herrero, R., Bambo, M.P., Pablo, L.E., and Fernandez, F.J. (2013). Use of Fourier-domain OCT to detect retinal nerve fiber layer degeneration in Parkinson's disease patients. Eye (Lond) *27*, 507-514.

Yatsuga, S., Povalko, N., Nishioka, J., Katayama, K., Kakimoto, N., Matsuishi, T., Kakuma, T., and Koga, Y. (2012). MELAS: a nationwide prospective cohort study of 96 patients in Japan. Biochim Biophys Acta *1820*, 619-624.